Electronic Supplementary Material (ESI) for RSC Advances.

Electronic Supplementary Information

Electrochemically dealloyed nanoporous $Fe_{40}Ni_{20}Co_{20}P_{15}C_5$ metallic glass for efficient and stable electrocatalytic hydrogen and oxygen generation

K.S Aneeshkumar [a,b], Jo-chi Tseng [a], Xiaodi Liu [a], Jinsen Tian [a,], Dongfeng Diao [a], Jun Shen [a,*]*

[a] College of Mechatronics and Control Engineering, Shenzhen University, Shenzhen 518060, China

[b] College of Physics and Optoelectronic Engineering, Shenzhen University, Shenzhen, 518060, China

Materials and methods

Experimental section

$Fe_{40}Ni_{20}Co_{20}P_{15}C_5$ master alloy ingots were prepared by arc melting high purity iron (Fe), Cobalt (Co), Nickel (Ni), Carbon (C), Fe_3P, and Ni_2P in a high purity argon atmosphere with Ti gettering. Fe_3P and Ni_2P compounds were used since phosphorous (P) are highly volatile in room temperature conditions. The stoichiometric equation for calculating the mass of raw materials for developing alloy ingot for $Fe_{40}Ni_{20}Co_{20}P_{15}C_5$ is given as $25\ Fe + 5Fe_3P + 10\ Ni_2P + 20\ Co + 5C \rightarrow Fe_{40}Ni_{20}Co_{20}P_{15}C_5$. Each alloy ingots were remelted four times to ensure homogenous chemical composition throughout the whole ingot. The metallic glass amorphous ribbons were prepared by remelting the as-prepared alloy ingots and suddenly spraying the melt through a tube nozzle over a copper roller which is rotating at high speed. Thus the melt was rolled into ribbons of width 3mm and thickness 25 μm.

Materials characterization

The microstructural phase composition of the metallic glass ribbons was characterized by X-ray diffraction (XRD) using a Bruker D8 Advance high-resolution diffractometer with Cu Kα radiation ($\lambda = 1.5406\ A^0$, 40 k V and 40 mA). Surface morphology was analyzed using a scanning electron microscope (SEM: FEI Quanta 450FEG), Transmission electron microscope (TEM: JEM-2100F), and elemental analysis was carried out using Energy Dispersive analysis of X-ray (EDX) spectrometer attached to TEM and SEM. The temperatures associated with thermal transitions were obtained using the differential scanning calorimeter, DSC instrument (Perkin Elmer DSC 8000) at a heating rate of 5K/min under N_2 atmosphere. X-ray photoelectron spectroscopy (XPS-thermos K-Alpha+) was used to investigate the chemical states for the as-prepared MG ribbon and the 20 hour tested MG ribbons.

Electrocatalytic measurements

The HER and OER electrochemical performance of the MG catalyst $Fe_{40}Ni_{20}Co_{20}P_{15}C_5$ were tested in a three-electrode configuration on a Gamry 600 plus electrochemical workstation (USA). Ag/AgCl and Hg/HgO electrode were used as a reference electrode in 0.5 M H_2SO_4 and 1M KOH, respectively, in acidic and alkaline media. Graphite carbon rod was used as the counter electrode in the acidic electrolyte, and a Pt tip electrode was used as a counter electrode in the alkaline electrolyte medium. The melt-spun ribbons were cut into 30 mm × 1 mm × 25 μm. The portion to be dipped in electrolyte solution was fixed as 0.4 cm, and the portion above the working part is wrapped by Teflon tape. It was assured that the electrolyte could not pass into the Teflon tape by properly pressing the Teflon tape. The active area of the metallic glass (MG) ribbon for electrochemical measurement is thus 0.08 cm^2. The ribbon samples were electrochemically dealloyed in 1M HCl by applying an optimized voltage of 0.2V for 30 minutes in a three-electrode configuration. After dealloying, samples were kept in a vacuum for 12 hours. The measurement for standard Pt and IrO_2 as working electrodes were prepared by dispersing 5mg of commercial Pt/C or IrO_2 powders in 650 μL deionized water and 350 μL isopropanol, 30 μL 5 wt% Nafion solution was added and sonicated for 30 min to form homogeneous dispersion. 5 μL ink was dropped on the surface of the GCE (surface area: 0.070685 cm^2) using a pipette and dried at 60 ^{0}C for 12 hr. Linear-sweep voltammetry with 95% iR compensation was carried out at a scan rate of 5 mV s^{-1} in 0.5 M H_2SO_4 and 1.0 M KOH, respectively. The linear sweep voltammetry (LSV) curves of each sample were measured five times, and the final cycle was always used for analysis. To determine the double layer capacitance per unit area (C_{dl}), a series cyclic voltammetry (CV) measurement was performed at various scan rates (200,150, 120, 100, 80, 60, 40, 20, and 10 mV.s^{-1}) in the non-faradaic region of polarization. The electrochemical active surface area, ECSA of the

MG electrocatalyst were calculated from the formula $ECSA = C_{dl}/C_s$, where C_s is the specific capacitance of an atomically smooth surface, 40 μF.cm^{-2}.[7] Electrochemical impedance spectra (EIS) were measured in the frequency range of 0.01 Hz to 10^5 Hz by applying a dc voltage at the corresponding overpotential,η_{10}. The long-term durability test of HER was determined by chronoamperometry at the corresponding overpotential,η_{10} and at a current density of 10 mA cm^{-2}. The cycling stability was tested by using Linear-sweep voltammetry after 2000 CV cycles with 100 mV s^{-1} in the voltage range 0 to 2V.

All the potentials in this study were compensated by iR_s as per the following equation (1):

$$E_{corr} = E_{meas} - iR_s(1) \quad (1)$$

of which, E_{corr} is compensated postpotential, E_{meas} is the measured potential during experiment and R_s is the solution resistance measured by electrochemical impedance spectroscopy (EIS).

All the potentials were converted into reversible hydrogen electrode potential (RHE) as per the following equation (2. a-c)

HER in Acid media: $E_{(vs\ RHE)} = E_{(vs\ Ag/AgCl)} + 0.059 \times pH\ (pH \sim 0) + 0.197\ V$ (2.a)

HER in alkaline media: $E_{(vs\ RHE)} = E_{(vs\ Hg/HgO)} + 0.059 \times pH\ (pH \sim 14) + 0.098\ V$ (2.b)

OER in alkaline media: $E_{(vs\ RHE)} = E_{(vs\ Hg/HgO)} + 0.059 \times pH\ (pH \sim 14) + 0.098\ V$ (2.c)

In 0.5M H_2SO_4 and 1M KOH, HER linear polarization curves were collected at a scan rate of 5 mV/s in the range of applied potential 0 to -2V vs. RHE. OER polarization curves were obtained at the same scan rate of 5 mV/s in the applied potential range 0 to 2V vs. RHE. The Tafel plot was derived from the corresponding LSV curve according to the Tafel equation (3):

$$\eta = a + b\log j \quad (3)$$

where 'η' represents the overpotential, 'b' is the Tafel slope, 'j' is the current density and 'a' is the exchange current density.

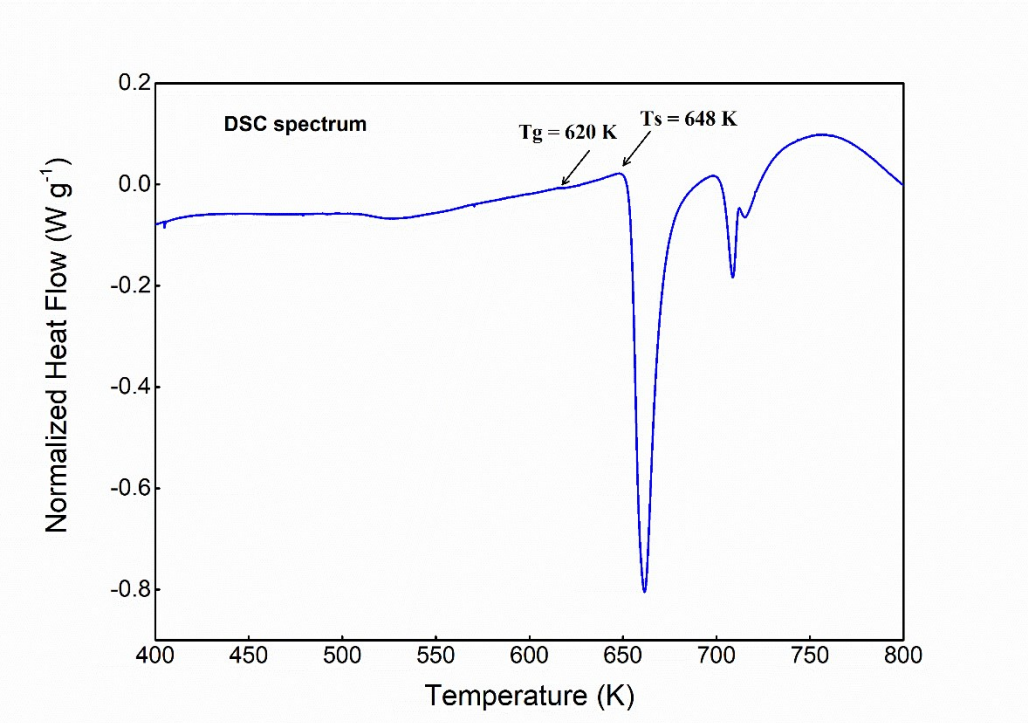

Fig. S1 DSC spectrum for MG ribbon.

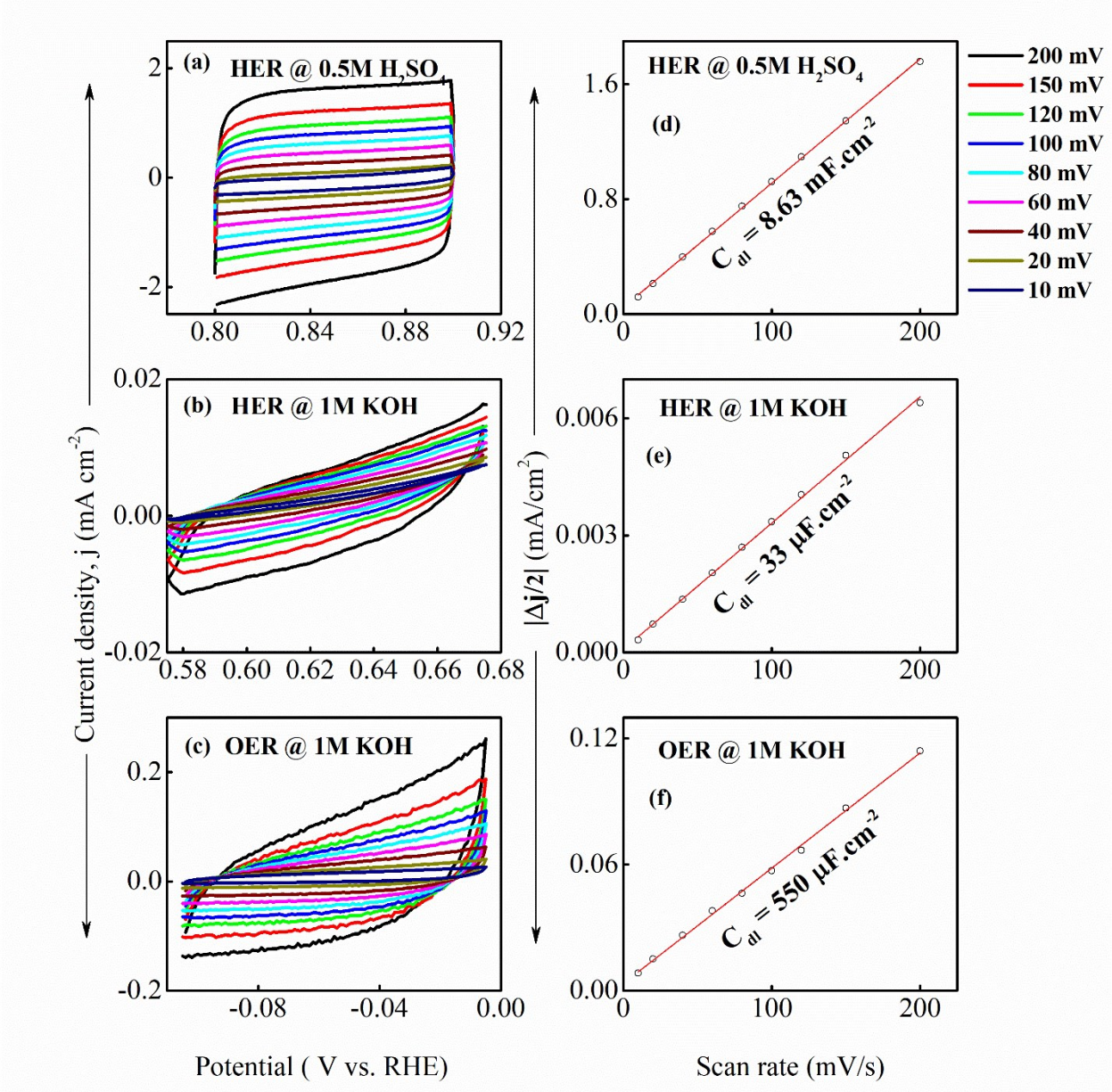

Fig. S2 CV curves of electrochemically dealloyed $Fe_{40}Co_{20}Ni_{20}P_{15}C_5$. (a) HER acidic, (b) HER alkaline, (c) OER alkaline (d-f) Corresponding plots showing the double-layer capacitance (C_{dl}) per unit area.

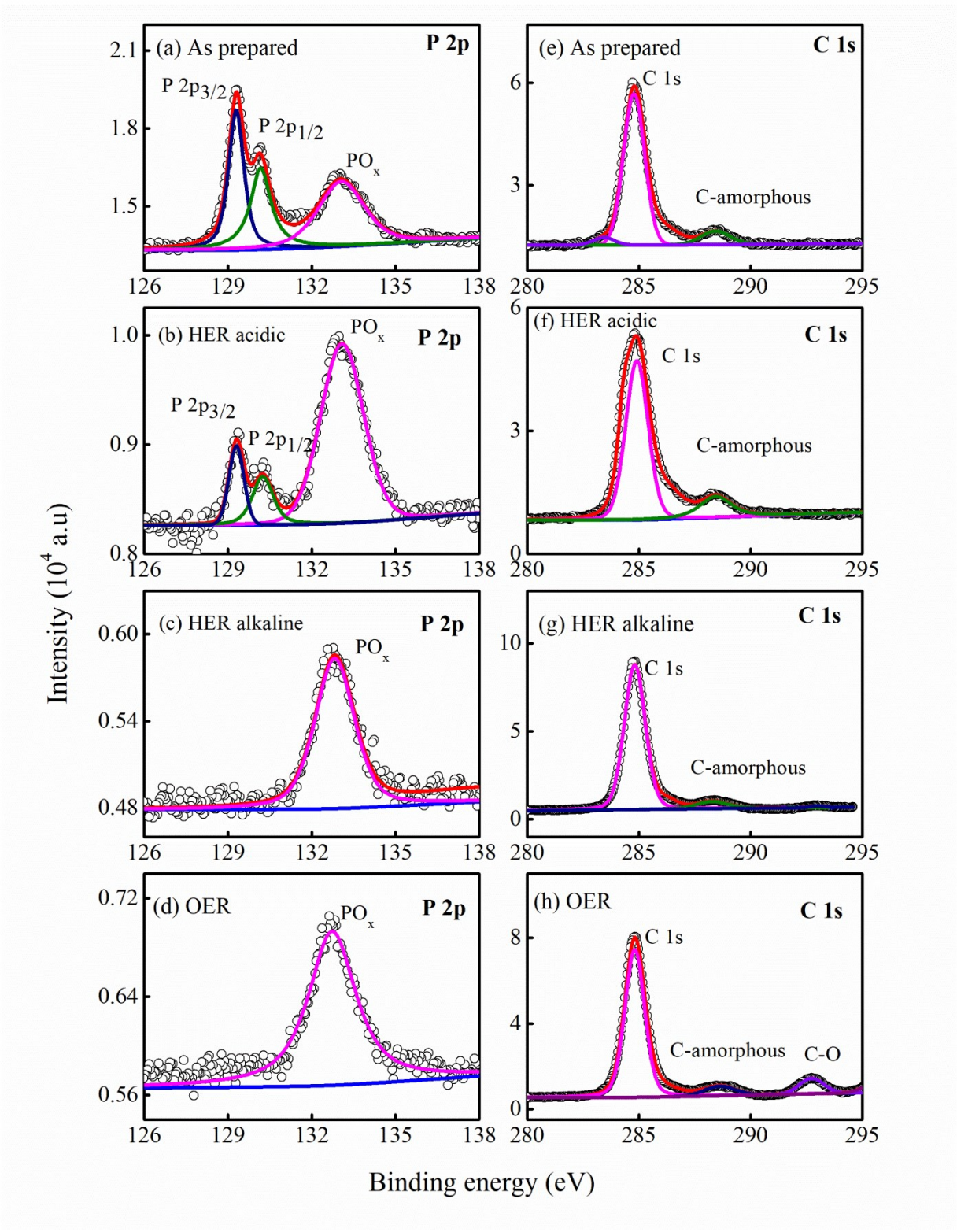

Fig. S3 XPS spectra before and after chronoamperometric tests. (a-d) XPS spectra for P 2p. (e-h) XPS spectra for C1s.

Table S1. HER performance of $Fe_{40}Ni_{20}Co_{20}P_{15}C_5$ MG and other reported electrocatalysts in acidic electrolytes.

Catalyst	Substrate	η_{10}/ mV	Tafel slope ($mV.dec^{-1}$)	Electrolyte	Ref.
Glassy $Fe_{40}Ni_{20}Co_{20}P_{15}C_5$/Dealloyed	Free-standing	128	67	0.5 M H_2SO_4	This work
10wt. % Pt/C	Glassy carbon	42	24	0.5 M H_2SO_4	This work
FeP porous nanosheet	Glassy carbon	240	67	0.5 M H_2SO_4	*Chem. Commun.* **2013**, *49*, 6656.
CoP/NTs	Glassy carbon	130	60	0.5 M H_2SO_4	*J. Mater. Chem. A* **2014**, *2*, 14812
NiCoP/rGO	Glassy carbon	59	51.2	0.5 M H_2SO_4	*Adv. Funct. Mater.* **2016**, *26*, 6785
FeCo@FeCoP@C	Glassy carbon	65	60	0.5 M H_2SO_4	*ACS Appl. Mater. Interfaces* **2019**, *11*, 1267
Fe@Fe_2P/NCNT	Glassy carbon	78.2	52.2	0.5 M H_2SO_4	*ChemElectroChem* **2019**, *6*, 1413
Ni_2P nanoparticles	Glassy carbon	187	16	0.5 M H_2SO_4	*J. Am. Chem. Soc.* **2013**, *135*, 9267
NiCoP nanowire	Glassy carbon	380	65	0.5 M H_2SO_4	*Mater. Res. Express* **2019**, *6* , 1150b3
Porous hollow NiCoP polyhedra	Glassy carbon	124	42	0.5 M H_2SO_4	*ACS Appl. Mater. Interfaces* **2017**, *9*, 5982
Mo_2C-porous	Glassy carbon	142	53	0.5 M H_2SO_4	*Nat. Commun.* **2015**, *6*, 6512
$Ni_{12}P_5$	Titanium foil	107	63	0.5 M H_2SO_4	*ACS Nano* **2014**, *8*, 8121
MoS_2 nanosheets	Glassy	180	55	0.5 M	*J. Am. Chem. Soc.*

	carbon			H_2SO_4	**2013**, *135* , 17881
$MoS_2/CoSe_2$	Glassy carbon	68	36	0.5 M H_2SO_4	*Nat. Commun.* **2015**, *6* , 5982
MoP nanoparticles	Glassy carbon	125	54	0.5 M H_2SO_4	*Adv. Mater.* **2014**, *26*, 5702
CoP nanoparticles	Glassy carbon	212.29	88.37	0.5 M H_2SO_4	*J. Mater. Chem. A* **2015**, *3*, 4255

Table S2. HER performance of $Fe_{40}Ni_{20}Co_{20}P_{15}C_5$ MG and other electrocatalysts in alkaline electrolytes.

Catalyst	substrate	η_{10}/ mV	Tafel slope (mV. dec^{-1})	Electroly-te	Ref.
Glassy $Fe_{40}Ni_{20}Co_{20}P_{15}C_5$ Dealloyed	Free-standing	236	110	1 M KOH	This work
Crystallized $Fe_{40}Ni_{20}Co_{20}P_{15}C_5$	Free-standing	312	95	1 M KOH	This work
10wt. % Pt/C	Glassy carbon	45	86	1 M KOH	This work
Ni/Mo_2C/ porous C	Nickel foam	179	101	1 M KOH	*J. Mater. Chem. A* 2015, 4255
FeP nanosheet/Ti	Ti	95	64	1 M KOH	*Appl. Catal. B Environ.* 2020, *260*, 118156
CoP	Carbon cloth	209	129	1 M KOH	*J. Am. Chem. Soc.* 2014, *136* (21), 7587
$NiCo_2P_x$ nanowire	Carbon fiber	58	34.3	1 M KOH	*Adv. Mater.* 2017, *29* (9), 1605502
Mo_2C-porous	Glassy carbon	151	59	1 M KOH	*Nat. Commun.* 2015, *6* (1), 6512
FeCoOH nanosheet	Nickel foam	126	N/A	1 M KOH	*Chem. – A Eur. J.* 2018, *24* (18), 4724
Ni/Mo_2C/ porous C	Glassy carbon	179	101	1 M KOH	*Chem. Sci.* 2016, *7* (5), 3399
$Co(OH)_2$@PANI	Nickel	88	91.6	1 M NaOH	*Adv. Mater.* 2015, *27*

	foam				(44), 7051
FeCoNiP@NC	Glassy carbon	187	52.2	1 M KOH	*Sustain. Energy Fuels* 2020, 4531
Glassy $Ni_{40}Fe_{40}P_{20}$	Free-standing	270	89	1 M KOH	*Adv. Mater. Interfaces* 2017, 1601086
Ni/NiO	Glassy carbon	90	101	1 M KOH	*Natl. Sci. Rev.* 2020, 27
FeP array	Glassy carbon	194	75	1 M KOH	*Chem. Commun.* 2016, 2819
FeP NAs/CC	Glassy carbon	218	146	1 M KOH	*ACS Catal.* 2014, 4065
MoB	Glassy carbon	225	59	1 M KOH	*Angew. Chemie Int. Ed.* 2012, *51*, 12703
FeP Nanotubes	Glassy carbon	120	60	1 M KOH	*Chem. – A Eur. J.* 2015, 18062

Table S3. OER performance of $Fe_{40}Ni_{20}Co_{20}P_{15}C_5$ MG and other reported high performing electrocatalysts in alkaline electrolytes.

Catalyst	substrate	η_{10}/ mV	Tafel slope (mV.dec^{-1})	Electrolyte	Reference
Glassy $Fe_{40}Ni_{20}Co_{20}P_{15}C_5$/ Dealloyed	Free-standing	278	40	1 M KOH	This work
Crystallized $Fe_{40}Ni_{20}Co_{20}P_{15}C_5$	Free-standing	365	44	1 M KOH	This work
IrO_2	Glassy carbon	385	90	1 M KOH	This work
Co-P	Co foil	345	47	1 M KOH	*Angew. Chemie Int. Ed.* 2015, 6251–6254
$Ni_xCo_{3-x}O_4$ nanowire	Glassy carbon	370	64	1 M KOH	*Angew. Chemie Int. Ed.* 2017,3897–3900
$NiFeO_x$	Carbon Fiber	230	31.5	1 M KOH	*Nat. Commun.* 2015, 7261
$(Fe_xNi_{1-x})P$	Nickel Foam	156	66	1 M KOH	*Nano Energy* 2017, *38*, 553
Ni-P nanosheet	Glassy carbon	300	64	1 M KOH	*Energy Environ. Sci.* 2016, 1246
NiCoP@C	Glassy carbon	297	58	1 M KOH	*Nanoscale* 2018, *10*, 13555
Ni-Co nanowire	Glassy carbon	302	43.6	1 M KOH	*Adv. Energy Mater.* 2017, 1601492
FeCoNiP@NC	Glassy carbon	266	35.6	1 M KOH	*Sustain. Energy Fuels* 2020, 4531

Glassy $Fe_{54}Ni_{30-x}Co_xNb_6B_9Cu_1$	Free-standing	274	37.4	1 M KOH	*J. Alloys Compd.* 2021, *852*, 156876
$NiCo_2O_4$/NiO	Glassy carbon	360	75	1 M KOH	*ACS Omega* 2017, *2*, 7559
NiCo-LDH	Nickel Foam	420	113	1 M KOH	*J. Power Sources* 2015, *278*, 445
MoO_2	Glassy carbon	330	78	1 M KOH	*J. Phys. Chem. C* 2020, *124*, 20010
NiFe Hydroxide	Glassy carbon	245	28	1 M KOH	*Nat. Commun.* 2015, *6*, 6616
NiCoFeP/C	Glassy carbon	270	65	1 M KOH	*Chem. Commun.* 2019, *55*, 10896
FeP/Fe_3O_4-CNT	Glassy carbon	229	27.6	1 M KOH	*ACS Appl. Mater. Interfaces* 2020, *12*, 12783